

# Tau neutrino helicity from $h^\pm$ energy correlations

CLEO Collaboration

## Abstract

We report a measurement of the magnitude of the tau neutrino helicity from tau-pair events taken with the CLEO detector at the CESR electron-positron storage ring. Events in which each tau undergoes the decay  $\tau \rightarrow h\nu$ , with  $h$  a charged pion or kaon, are analyzed for energy correlations between the daughter hadrons, yielding  $|\xi_h| = 1.03 \pm 0.06 \pm 0.04$ , with the first error statistical and the second systematic.

*Submitted to Physical Review D*

T. E. Coan,<sup>1</sup> V. Fadeyev,<sup>1</sup> I. Korolkov,<sup>1</sup> Y. Maravin,<sup>1</sup> I. Narsky,<sup>1</sup> V. Shelkov,<sup>1</sup> J. Staeck,<sup>1</sup>  
 R. Stroynowski,<sup>1</sup> I. Volobouev,<sup>1</sup> J. Ye,<sup>1</sup> M. Artuso,<sup>2</sup> A. Efimov,<sup>2</sup> F. Frascioni,<sup>2</sup> M. Gao,<sup>2</sup>  
 M. Goldberg,<sup>2</sup> D. He,<sup>2</sup> S. Kopp,<sup>2</sup> G. C. Moneti,<sup>2</sup> R. Mountain,<sup>2</sup> S. Schuh,<sup>2</sup> T. Skwarnicki,<sup>2</sup>  
 S. Stone,<sup>2</sup> G. Viehhauser,<sup>2</sup> X. Xing,<sup>2</sup> J. Bartelt,<sup>3</sup> S. E. Csorna,<sup>3</sup> V. Jain,<sup>3</sup> S. Marka,<sup>3</sup>  
 A. Freyberger,<sup>4</sup> R. Godang,<sup>4</sup> K. Kinoshita,<sup>4</sup> I. C. Lai,<sup>4</sup> P. Pomianowski,<sup>4</sup> S. Schrenk,<sup>4</sup>  
 G. Bonvicini,<sup>5</sup> D. Cinabro,<sup>5</sup> R. Greene,<sup>5</sup> L. P. Perera,<sup>5</sup> G. J. Zhou,<sup>5</sup> B. Barish,<sup>6</sup>  
 M. Chadha,<sup>6</sup> S. Chan,<sup>6</sup> G. Eigen,<sup>6</sup> J. S. Miller,<sup>6</sup> C. O'Grady,<sup>6</sup> M. Schmidtler,<sup>6</sup> J. Urheim,<sup>6</sup>  
 A. J. Weinstein,<sup>6</sup> F. Würthwein,<sup>6</sup> D. M. Asner,<sup>7</sup> D. W. Bliss,<sup>7</sup> W. S. Brower,<sup>7</sup> G. Masek,<sup>7</sup>  
 H. P. Paar,<sup>7</sup> V. Sharma,<sup>7</sup> J. Gronberg,<sup>8</sup> T. S. Hill,<sup>8</sup> R. Kutschke,<sup>8</sup> D. J. Lange,<sup>8</sup>  
 S. Menary,<sup>8</sup> R. J. Morrison,<sup>8</sup> H. N. Nelson,<sup>8</sup> T. K. Nelson,<sup>8</sup> C. Qiao,<sup>8</sup> J. D. Richman,<sup>8</sup>  
 D. Roberts,<sup>8</sup> A. Ryd,<sup>8</sup> M. S. Witherell,<sup>8</sup> R. Balest,<sup>9</sup> B. H. Behrens,<sup>9</sup> K. Cho,<sup>9</sup> W. T. Ford,<sup>9</sup>  
 H. Park,<sup>9</sup> P. Rankin,<sup>9</sup> J. Roy,<sup>9</sup> J. G. Smith,<sup>9</sup> J. P. Alexander,<sup>10</sup> C. Bebek,<sup>10</sup> B. E. Berger,<sup>10</sup>  
 K. Berkelman,<sup>10</sup> K. Bloom,<sup>10</sup> D. G. Cassel,<sup>10</sup> H. A. Cho,<sup>10</sup> D. M. Coffman,<sup>10</sup>  
 D. S. Crowcroft,<sup>10</sup> M. Dickson,<sup>10</sup> P. S. Drell,<sup>10</sup> K. M. Ecklund,<sup>10</sup> R. Ehrlich,<sup>10</sup> R. Elia,<sup>10</sup>  
 A. D. Foland,<sup>10</sup> P. Gaidarev,<sup>10</sup> R. S. Galik,<sup>10</sup> B. Gittelmann,<sup>10</sup> S. W. Gray,<sup>10</sup> D. L. Hartill,<sup>10</sup>  
 B. K. Heltsley,<sup>10</sup> P. I. Hopman,<sup>10</sup> J. Kandaswamy,<sup>10</sup> N. Katayama,<sup>10</sup> P. C. Kim,<sup>10</sup>  
 D. L. Kreinick,<sup>10</sup> T. Lee,<sup>10</sup> Y. Liu,<sup>10</sup> G. S. Ludwig,<sup>10</sup> J. Masui,<sup>10</sup> J. Mevissen,<sup>10</sup>  
 N. B. Mistry,<sup>10</sup> C. R. Ng,<sup>10</sup> E. Nordberg,<sup>10</sup> M. Ogg,<sup>10,\*</sup> J. R. Patterson,<sup>10</sup> D. Peterson,<sup>10</sup>  
 D. Riley,<sup>10</sup> A. Soffer,<sup>10</sup> C. Ward,<sup>10</sup> M. Athanas,<sup>11</sup> P. Avery,<sup>11</sup> C. D. Jones,<sup>11</sup> M. Lohner,<sup>11</sup>  
 C. Prescott,<sup>11</sup> J. Yelton,<sup>11</sup> J. Zheng,<sup>11</sup> G. Brandenburg,<sup>12</sup> R. A. Briere,<sup>12</sup> Y. S. Gao,<sup>12</sup>  
 D. Y.-J. Kim,<sup>12</sup> R. Wilson,<sup>12</sup> H. Yamamoto,<sup>12</sup> T. E. Browder,<sup>13</sup> F. Li,<sup>13</sup> Y. Li,<sup>13</sup>  
 J. L. Rodriguez,<sup>13</sup> T. Bergfeld,<sup>14</sup> B. I. Eisenstein,<sup>14</sup> J. Ernst,<sup>14</sup> G. E. Gladding,<sup>14</sup>  
 G. D. Gollin,<sup>14</sup> R. M. Hans,<sup>14</sup> E. Johnson,<sup>14</sup> I. Karliner,<sup>14</sup> M. A. Marsh,<sup>14</sup> M. Palmer,<sup>14</sup>  
 M. Selen,<sup>14</sup> J. J. Thaler,<sup>14</sup> K. W. Edwards,<sup>15</sup> A. Bellerive,<sup>16</sup> R. Janicek,<sup>16</sup>  
 D. B. MacFarlane,<sup>16</sup> K. W. McLean,<sup>16</sup> P. M. Patel,<sup>16</sup> A. J. Sadoff,<sup>17</sup> R. Ammar,<sup>18</sup>  
 P. Baringer,<sup>18</sup> A. Bean,<sup>18</sup> D. Besson,<sup>18</sup> D. Coppage,<sup>18</sup> C. Darling,<sup>18</sup> R. Davis,<sup>18</sup>  
 N. Hancock,<sup>18</sup> S. Kotov,<sup>18</sup> I. Kravchenko,<sup>18</sup> N. Kwak,<sup>18</sup> S. Anderson,<sup>19</sup> Y. Kubota,<sup>19</sup>  
 M. Lattery,<sup>19</sup> S. J. Lee,<sup>19</sup> J. J. O'Neill,<sup>19</sup> S. Patton,<sup>19</sup> R. Poling,<sup>19</sup> T. Riehle,<sup>19</sup> V. Savinov,<sup>19</sup>  
 A. Smith,<sup>19</sup> M. S. Alam,<sup>20</sup> S. B. Athar,<sup>20</sup> Z. Ling,<sup>20</sup> A. H. Mahmood,<sup>20</sup> H. Severini,<sup>20</sup>  
 S. Timm,<sup>20</sup> F. Wappler,<sup>20</sup> A. Anastassov,<sup>21</sup> S. Blinov,<sup>21,†</sup> J. E. Duboscq,<sup>21</sup> K. D. Fisher,<sup>21</sup>  
 D. Fujino,<sup>21,‡</sup> R. Fulton,<sup>21</sup> K. K. Gan,<sup>21</sup> T. Hart,<sup>21</sup> K. Honscheid,<sup>21</sup> H. Kagan,<sup>21</sup> R. Kass,<sup>21</sup>  
 J. Lee,<sup>21</sup> M. B. Spencer,<sup>21</sup> M. Sung,<sup>21</sup> A. Undrus,<sup>21,†</sup> R. Wanke,<sup>21</sup> A. Wolf,<sup>21</sup>  
 M. M. Zoeller,<sup>21</sup> B. Nematy,<sup>22</sup> S. J. Richichi,<sup>22</sup> W. R. Ross,<sup>22</sup> P. Skubic,<sup>22</sup> M. Wood,<sup>22</sup>  
 M. Bishai,<sup>23</sup> J. Fast,<sup>23</sup> E. Gerndt,<sup>23</sup> J. W. Hinson,<sup>23</sup> N. Menon,<sup>23</sup> D. H. Miller,<sup>23</sup>  
 E. I. Shibata,<sup>23</sup> I. P. J. Shipsey,<sup>23</sup> M. Yurko,<sup>23</sup> L. Gibbons,<sup>24</sup> S. D. Johnson,<sup>24</sup> Y. Kwon,<sup>24</sup>  
 S. Roberts,<sup>24</sup> E. H. Thorndike,<sup>24</sup> C. P. Jessop,<sup>25</sup> K. Lingel,<sup>25</sup> H. Marsiske,<sup>25</sup> M. L. Perl,<sup>25</sup>  
 S. F. Schaffner,<sup>25</sup> D. Ugolini,<sup>25</sup> R. Wang,<sup>25</sup> and X. Zhou<sup>25</sup>

---

\*Permanent address: University of Texas, Austin TX 78712

†Permanent address: BINP, RU-630090 Novosibirsk, Russia.

‡Permanent address: Lawrence Livermore National Laboratory, Livermore, CA 94551.

- <sup>1</sup>Southern Methodist University, Dallas, Texas 75275  
<sup>2</sup>Syracuse University, Syracuse, New York 13244  
<sup>3</sup>Vanderbilt University, Nashville, Tennessee 37235  
<sup>4</sup>Virginia Polytechnic Institute and State University, Blacksburg, Virginia 24061  
<sup>5</sup>Wayne State University, Detroit, Michigan 48202  
<sup>6</sup>California Institute of Technology, Pasadena, California 91125  
<sup>7</sup>University of California, San Diego, La Jolla, California 92093  
<sup>8</sup>University of California, Santa Barbara, California 93106  
<sup>9</sup>University of Colorado, Boulder, Colorado 80309-0390  
<sup>10</sup>Cornell University, Ithaca, New York 14853  
<sup>11</sup>University of Florida, Gainesville, Florida 32611  
<sup>12</sup>Harvard University, Cambridge, Massachusetts 02138  
<sup>13</sup>University of Hawaii at Manoa, Honolulu, Hawaii 96822  
<sup>14</sup>University of Illinois, Champaign-Urbana, Illinois 61801  
<sup>15</sup>Carleton University, Ottawa, Ontario, Canada K1S 5B6  
and the Institute of Particle Physics, Canada  
<sup>16</sup>McGill University, Montréal, Québec, Canada H3A 2T8  
and the Institute of Particle Physics, Canada  
<sup>17</sup>Ithaca College, Ithaca, New York 14850  
<sup>18</sup>University of Kansas, Lawrence, Kansas 66045  
<sup>19</sup>University of Minnesota, Minneapolis, Minnesota 55455  
<sup>20</sup>State University of New York at Albany, Albany, New York 12222  
<sup>21</sup>Ohio State University, Columbus, Ohio 43210  
<sup>22</sup>University of Oklahoma, Norman, Oklahoma 73019  
<sup>23</sup>Purdue University, West Lafayette, Indiana 47907  
<sup>24</sup>University of Rochester, Rochester, New York 14627  
<sup>25</sup>Stanford Linear Accelerator Center, Stanford University, Stanford, California 94309

In the Standard Model of the weak interaction the tau is a sequential lepton with a purely left-handed weak isodoublet partner,  $\nu_\tau$ ; i.e., the tau neutrino has its spin anti-parallel to its momentum. For the decay of the tau to a single pseudoscalar hadron  $h$  (with  $h = \pi$  or  $K$ ), the parent tau spin is maximally correlated with the daughter hadron direction [1]. At high beam energies, the  $s$ -channel interaction  $e^+e^- \rightarrow \gamma^* \rightarrow \tau^+\tau^- \rightarrow (h^+\bar{\nu})(h^-\nu)$  tends to have the tau spins aligned, leading to a correlation between the angles of the hadron momentum vectors as measured in the tau rest frames. The Lorentz boost to the laboratory frame also maps these angles into the observed particle energies, transforming the spin-direction correlation into an energy-energy correlation between the hadrons. In this Brief Report we describe a measurement of the magnitude of the tau neutrino helicity based on pseudoscalar energy-energy correlations at a center-of-mass energy of  $\sqrt{s}=2E_b \simeq 10.6$  GeV. This study complements other recent measurements that involve other modes, other techniques, and/or higher beam energies [2–6].

The helicity, denoted here as  $\xi_h$  and elsewhere as  $h_{\nu_\tau}$ , is related to the parameter  $\gamma_{av}$  and the charged current couplings  $g_a$  and  $g_v$  by [7–9]

$$\xi_h = h_{\nu_\tau} = -\gamma_{av} = -2g_a g_v / (g_a^2 + g_v^2) \quad (1)$$

If we define  $c_\pm$  as the cosine of the angle of the  $h^\pm$  momentum in the parent rest frame with respect to the boost direction, the correlation is given by [7]

$$\frac{d^2\sigma}{dc_+dc_-} \propto 1 + \frac{(2E_b^2 - m_\tau^2)}{(2E_b^2 + m_\tau^2)} \xi_h^2 c_+ c_- . \quad (2)$$

At  $\sqrt{s}=10.6$  GeV, the net spin alignment is roughly 90%. Using instead the laboratory variables  $x_\pm = \sqrt{p_\pm^2 + m_\pi^2}/E_b$  gives the energy-energy correlation [8,9]

$$\frac{d^2\sigma}{dx_+dx_-} = F_1(x_+, x_-) + \xi_h^2 \cdot F_2(x_+, x_-), \quad (3)$$

with  $F_{1,2}$  being known kinematic functions. This correlation is maximal and identical for a left-handed ( $\xi_h=-1$ ) and a right-handed ( $\xi_h=+1$ ) tau neutrino, and it vanishes for no preferred handedness ( $\xi_h=0$ ). It is not explicitly parity-violating but is a consequence of parity violation in tau decay.

The data analyzed here correspond to a luminosity of  $1.64 \text{ fb}^{-1}$  ( $1.5 \times 10^6$   $\tau^+\tau^-$  events), collected at the Cornell Electron Storage Ring (CESR) with the CLEO II detector [10]. A set of three concentric drift chambers in a 1.5 T axial magnetic field measures charged particle momenta with resolution  $\sigma_p/p$  (%)  $\simeq \sqrt{(0.15p)^2 + (0.5)^2}$ ,  $p$  in GeV/ $c$ . Surrounding the drift chambers, but inside the superconducting magnet coil, is a CsI(Tl) crystal electromagnetic calorimeter. Barrel crystals surround the tracking chambers, covering  $|\cos\theta| < 0.82$ , with  $\theta$  the angle with respect to the  $e^+$  beam direction. Two identical endcaps occupy  $0.80 < |\cos\theta| < 0.98$ . Particle time-of-flight is provided by 5 cm-thick scintillation counters located just inside the calorimeter in the barrel and endcap. Muons are identified by their penetration through the calorimeter, coil and one or more of three 36 cm-thick slabs of magnet iron; three layers of Iarocci tube chambers instrument the gap behind each slab. A three stage hardware trigger [11] uses combinations of calorimeter, tracking chamber, and time-of-flight information to initiate detector readout.

To measure  $|\xi_h|$  we first extract  $\tau^+\tau^- \rightarrow (h^+\bar{\nu})(h^-\nu)$  events that are relatively free of backgrounds from non-tau processes. Monte Carlo samples of events from  $V$  and  $V\pm A$  processes are then generated and mixed appropriately to obtain a desired value of  $\xi_h$ . We determine what value of  $\xi_h$  best fits the data using likelihood and  $\chi^2$  methods, investigating both two-dimensional  $(x_+, x_-)$  and one-dimensional  $(c_+c_-)$  distributions. The techniques are then analyzed for systematic biases and uncertainties.

Events are selected that have exactly two oppositely charged tracks in the fiducial volume of the tracking system with  $|\cos\theta|<0.7$  and  $x_{\pm}>0.2$  and which project back to the  $e^+e^-$  luminous region. To reduce the contamination of non- $\tau\tau$  QED events, we demand that at most one track have  $x_{\pm}>0.8$ , that neither track have  $x_{\pm}>0.95$ , and that the total shower energy in the calorimeter be less than  $0.85\sqrt{s}$ . To remove backgrounds from final states that involve electrons, each track must have its calorimeter energy less than 85% of its measured momentum. These criteria reduce the number of events to about 115,000.

Final states that contain photons from neutral pions are suppressed by demanding that there be no photon-like showers in the calorimeter that are not matched to charged tracks. A combination of energy and isolation criteria is used to identify such showers. This requirement also greatly reduces the contamination from events with a single photon, such as from the process  $e^+e^- \rightarrow \rho\gamma$ . To suppress these radiative events further the two charged tracks are required to have an opening angle of greater than  $90^\circ$  in the  $r - \phi$  projection. To minimize possible systematic effects, events must satisfy trigger criteria that are suitable for two-track events and that are uniform throughout the dataset.

The most effective variable for removing events from  $\gamma\gamma$  interactions is  $\Theta_{\min}$ , defined by

$$\sin\Theta_{\min} = \frac{|\vec{p}_{\perp}|}{E_b \cdot (2 - x_- - x_+)}, \quad (4)$$

i.e., the ratio of  $|\vec{p}_{\perp}|$ , the missing net momentum transverse to the beams, to the missing energy of the event [12,13]. This requirement also effectively suppresses radiative QED events in which radiated photons go undetected. Events are retained if  $\sin\Theta_{\min}>0.10$ . Because particles from  $\gamma\gamma$  interactions tend to have low momentum, at least one of the tracks is also required to have  $x_{\pm}>0.3$ .

Discrimination against muons involves four mutually exclusive criteria, three of which use information from the muon chambers and one of which demands the particle leave an energy deposition in the calorimeter that is inconsistent in magnitude and shape with that of a muon. This last criterion is invoked only if the charged track projects into uninstrumented regions at the azimuthal boundaries of the iron absorber. Each track must pass one of these four criteria for the event to be accepted. The efficiency of the combination of these criteria to select a track as a pion has been measured using an independent subsample of hadrons in  $\tau^+\tau^-$  decays involving a lepton recoiling against one or more neutral pions and a single track that is assumed to be a charged pion or kaon ( $\ell - h(n\pi^0)$ ). This efficiency rises sharply from a threshold at  $x_{\pm} \sim 0.2$  to 60% at  $x_{\pm} \sim 0.25$ , and reaches a plateau of about 70% by  $x_{\pm} \sim 0.5$ . Studies of radiative mu-pair ( $\mu\mu\gamma$ ) events in both data and simulation indicate a rate for misidentification of a muon as a pion of less than 2% per track over the kinematic range of this analysis.

The resulting 2041  $h^+h^-$  candidates are binned in  $x_+$  vs.  $x_-$  with bin size 0.1 and range  $0.2 < x_{\pm} < 0.95$ , as shown in Fig. 1. The missing corner bins at  $x_+=x_-$  are the result of the

energy criteria that help suppress  $\gamma\gamma$  events and QED events. This figure clearly shows the depletion in the other corners that have one “hard” and one “soft” hadron, as expected for  $V \pm A$ . In addition we examine the product  $c_+c_-$  as shown in Fig. 2.

The Monte Carlo simulations start with the KORALB [14] tau-pair generator and use the GEANT package [15] to model the detector response. Monte Carlo studies indicate that over 97% of these events were of the five final states  $\pi^+\pi^-\nu\bar{\nu}$  (81%),  $\pi^\pm K^\mp\nu\bar{\nu}$  (9%),  $\pi^\pm\rho^\mp\nu\bar{\nu}$  (4%),  $\pi^\pm\mu^\mp\nu\bar{\nu}(\nu/\bar{\nu})$  (2%), and  $\pi^\pm K^{*\mp}\nu\bar{\nu}$  (2%); the next leading mode was  $\pi^\pm e^\mp\nu\bar{\nu}(\nu/\bar{\nu})$  (0.8%). For these five specific decay channels large samples were generated with both  $(V-A)$  and pure  $V$  coupling. In the case of  $\pi^\pm\mu^\mp\nu\bar{\nu}(\nu/\bar{\nu})$  events were also thrown with a  $(V+A)$  coupling; for the other final states the  $(V+A)$  and  $(V-A)$  predictions are identical. These events are then appropriately scaled to be added together for comparison to the data distributions. For each bin in either the  $(x_+, x_-)$  or  $c_+c_-$  analysis, the number of predicted events for *any* given value of  $\xi_h$  is expressed in terms of the number from the  $(V-A)$ ,  $(V+A)$  and  $V$  simulations by

$$n_i(\xi_h) = C_{-1}N_i^{V-A} + C_{+1}N_i^{V+A} + C_0N_i^V \quad (5)$$

with  $C_{\pm 1} = (\xi_h^2 \pm \xi_h)/2$  and  $C_0 = (1 - \xi_h^2)$ . A binned maximum likelihood fit in the one parameter,  $\xi_h$ , is then performed, with the resulting likelihood distribution for the  $(x_+, x_-)$  analysis shown in Fig. 3. The result is  $|\xi_h| = 0.998_{-0.059}^{+0.063}$ , with the uncertainty being purely statistical. A similar likelihood curve is found for the  $c_+c_-$  analysis [16], yielding  $|\xi_h| = 1.011_{-0.060}^{+0.064}$ .

We have made many systematic checks which can be divided into four broad categories: possible biases in the methodology, our estimate of backgrounds, dependence on the simulation of the variables used in event selection, and possible biases in the simulations. These systematic effects have been studied for both the  $(x_+, x_-)$  and  $c_+c_-$  analyses. Because the values of  $|\xi_h|$  from the two analyses are statistically indistinguishable, only the details for the  $(x_+, x_-)$  analysis will be given.

In addition to the likelihood technique, a  $\chi^2$  analysis was performed, with minimal shift in the value of  $|\xi_h|$ . Further, studies with very large samples of simulated events (which, for speed, had their kinematic variables smeared with typical resolution functions instead of full detector simulation) showed that the choice of the likelihood estimator causes no inherent shift in the value of  $|\xi_h|$ . Various choices of bin size were tried for both the likelihood and  $\chi^2$  analyses, from which we assign a systematic uncertainty of  $\pm 0.02$ .

Studies with Monte Carlo samples indicate a bias of  $-0.011 \pm 0.006$  in the fitting procedure and of  $-0.020 \pm 0.010$  due to the use of only the five most common modes. We include these shifts to obtain a central value of  $|\xi_h| = 1.029$  and incorporate the uncertainties on the shifts into the overall systematic error.

If the Monte Carlo were not properly handling the various  $\tau^+\tau^-$  decays or if there were non-trivial amounts of non-tau backgrounds, then changing the tau branching fractions would affect the result because the various final states have different distributions in the  $(x_+, x_-)$  plane. Variations of 10-20% in these branching fractions produced changes in  $|\xi_h|$  of less than 0.01. We used an extended likelihood technique to incorporate the normalization into the fit, which yielded a tau branching fraction and statistical uncertainty of  $\mathcal{B}_\tau = 0.11 \pm 0.01$ , consistent with the established value [13,17]. This extension of the likelihood to include normalization had a negligible effect on the fitted value of  $|\xi_h|$ , changing it by 0.01.

The effect of possible contamination from the  $\mu\mu\gamma$  final state was investigated by introducing simulated  $\mu\mu(\gamma)$  events into the data sample. After weighting events that passed all but the muon rejection criteria by roughly five times the rate at which muons fake hadrons, a shift in  $\xi_h$  of  $-0.02$  is observed. The resulting uncertainty on  $|\xi_h|$ , assuming the actual measured misidentification rate, is less than 0.005.

The Monte Carlo simulations for the final state  $\pi^+\pi^-\nu\bar{\nu}$  were examined to see if any of the efficiencies of the various selection criteria were different for  $V$  and  $V-A$ . Of all the selection criteria, the restriction on  $\sin\Theta_{\min}$  is the one to which  $\xi_h$  is most sensitive, especially because it tends to eliminate events along the diagonal in the  $(x_+, x_-)$  plane. We therefore varied the limit on  $\sin\Theta_{\min}$  down to 0.05 and up to 0.20, observing changes in the fitted value of  $<0.02$ . Replacing the limit on  $\sin\Theta_{\min}$  with requirements on acoplanarity or visible event energy (also effective in suppressing  $\gamma\gamma$  backgrounds, but less so) produced similar changes in  $|\xi_h|$ , but of the opposite sign. An uncertainty of  $\pm 0.01$  was assigned to this effect.

Other event selection variables were also evaluated by varying the requirements, leading to very small uncertainties. An exception was the  $h/\mu$  discrimination, for which we tried using various subsets of the four criteria as well as changing the limits in them individually, leading to an associated uncertainty of  $\pm 0.025$ . Similarly we tightened and loosened (where possible) the trigger requirements with effects observed of  $\pm 0.015$ .

All of the efficiencies depend on the Monte Carlo simulations. The most critical aspects of this are the photon veto (for which hadronic splittings need to be properly modeled), the  $h/\mu$  discrimination, and the trigger. To investigate these more thoroughly, samples of events were obtained in both data and in Monte Carlo simulation for the  $\ell-h(n\pi^0)$  topology previously described. From these studies we obtained  $x_{\pm}$ -dependent corrections to the efficiencies for all three aspects of the analysis. Applying these indicated very small shifts, some positive and some negative, in the fitted value of  $|\xi_h|$ . Based on this we applied no shift in the central value and assigned a systematic uncertainty of  $\pm 0.01$ .

Taking all the effects in quadrature yields an overall systematic uncertainty of  $\Delta\xi_h = \pm 0.040$  for the  $(x_+, x_-)$  analysis. For the  $c_+c_-$  analysis, the biases shift the central value to  $|\xi_h| = 1.036$  with a systematic uncertainty of  $\Delta\xi_h = \pm 0.049$ . Our quoted value for the helicity and its uncertainties is the simple average of these two analyses.

In summary, we have measured the magnitude of the helicity of the tau neutrino from the energy-energy correlation in  $\tau^+\tau^-\rightarrow(h^+\bar{\nu})(h^-\nu)$  events, obtaining  $|\xi_h|=1.03\pm 0.06\pm 0.04$ . This is consistent with the other measures of the  $\nu_\tau$  helicity [2–6]. Considering only  $V$  and  $A$  interactions, the physical bounds are  $0<|\xi_h|<1$ , and our result corresponds to  $|\xi_h|>0.87$  at 95%CL. From Eqn. 5 this implies at most 24% pure  $V$  (or pure  $A$ ) at 95% CL.

We gratefully acknowledge the effort of the CESR staff in providing us with excellent luminosity and running conditions. This work was supported by the National Science Foundation, the U.S. Department of Energy, the Heisenberg Foundation, the Alexander von Humboldt Stiftung, Research Corporation, the Natural Sciences and Engineering Research Council of Canada, and the A.P. Sloan Foundation.

## REFERENCES

- [1] Y.S. Tsai, Phys. Rev. D **4**, 2821 (1971); Phys. Rev. D **13**, 771(E) (1976).
- [2] ARGUS Collaboration, H. Albrecht *et al.*, Z. Phys. C **58**, 61 (1993). Using asymmetries in  $hh\nu$  decays, the signed result is  $\xi = -1.25 \pm 0.23 \begin{smallmatrix} +0.15 \\ -0.08 \end{smallmatrix}$ .
- [3] ARGUS Collaboration, H. Albrecht *et al.*, Phys. Lett. B **337**, 383 (1994). Using the final state  $\rho\nu$  yielded  $|\xi_h| = 1.022 \pm 0.028 \pm 0.030$ .
- [4] ALEPH Collaboration, D. Buskulic *et al.*, Phys. Lett. B **346**, 379 (1995); **B 363**, 265 (E) (1995). For the  $\pi\nu$  mode their result is  $|\xi_h| = 0.987 \pm 0.057 \pm 0.027$ ; combining all modes the ALEPH result is  $|\xi_h| = 1.006 \pm 0.032 \pm 0.019$ .
- [5] L3 Collaboration, M. Acciarri *et al.*, Phys. Lett. B **377**, 313 (1996). Averaging over  $\pi\nu$  and  $\rho\nu$  decays produced a value of  $|\xi_h| = 0.973 \pm 0.053 \pm 0.011$ .
- [6] OPAL Collaboration, R. Akers *et al.*, Z. Phys. C **67**, 45 (1995). Using asymmetries in  $hh\nu$  decays yielded the signed result of  $\xi = -1.08 \begin{smallmatrix} +0.46 & +0.14 \\ -0.41 & -0.25 \end{smallmatrix}$ .
- [7] J.H. Kühn and F. Wagner, Nucl. Phys. **B236**, 16 (1984).
- [8] C. Nelson, Phys. Rev. D **43**, 1465 (1991).
- [9] W. Fetscher, Phys. Rev. D **42**, 1544 (1990).
- [10] CLEO Collaboration, Y. Kubota *et al.*, Nucl. Instrum. Methods Phys. Res., Sect. A **320**, 66 (1992).
- [11] C. Bebek *et al.*, Nucl. Instrum. Methods Phys. Res., Sect. A **302**, 261 (1991).
- [12] J. Masui, Ph.D. Thesis, Cornell University, 1997.
- [13] CLEO Collaboration, A. Anastassov *et al.*, CLNS 96/1431 (to be published in PRD).
- [14] S. Jadach and Z. Was, Comp. Phys. Comm. **36**, 191 (1985); **64**, 267 (1991); S. Jadach, J.H. Kühn, and Z. Was, *ibid.* **64**, 275 (1991); **70**, 69 (1992); **76**, 361 (1993).
- [15] R. Brun *et al.*, *GEANT v.3.15*, CERN DD/EE/84-1, 1987 (unpublished).
- [16] Using the mean of this distribution, i.e.,  $\langle c_+c_- \rangle$ , as the estimator gives  $|\xi_h| = 1.05 \pm 0.06$ . No systematic study of this zero-dimensional analysis was performed.
- [17] Particle Data Group, R.M. Barnett *et al.*, Phys. Rev. D **54**, Part I (1996).



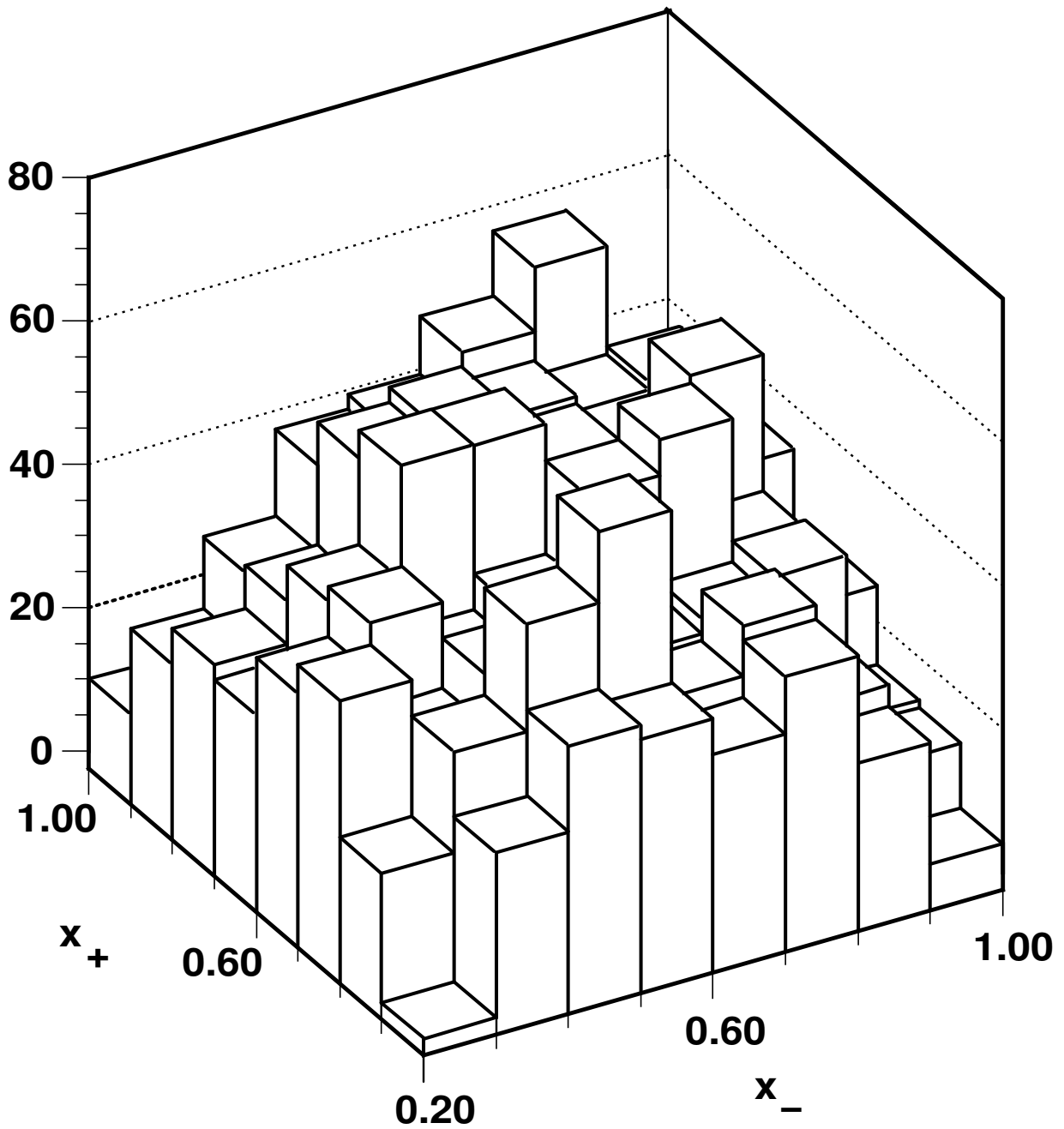


FIG. 1. The energy-energy distribution for the data, uncorrected for efficiencies, using the scaled energy variables. Note that the actual range of the data is  $0.2 < x_{\pm} < 0.95$ .

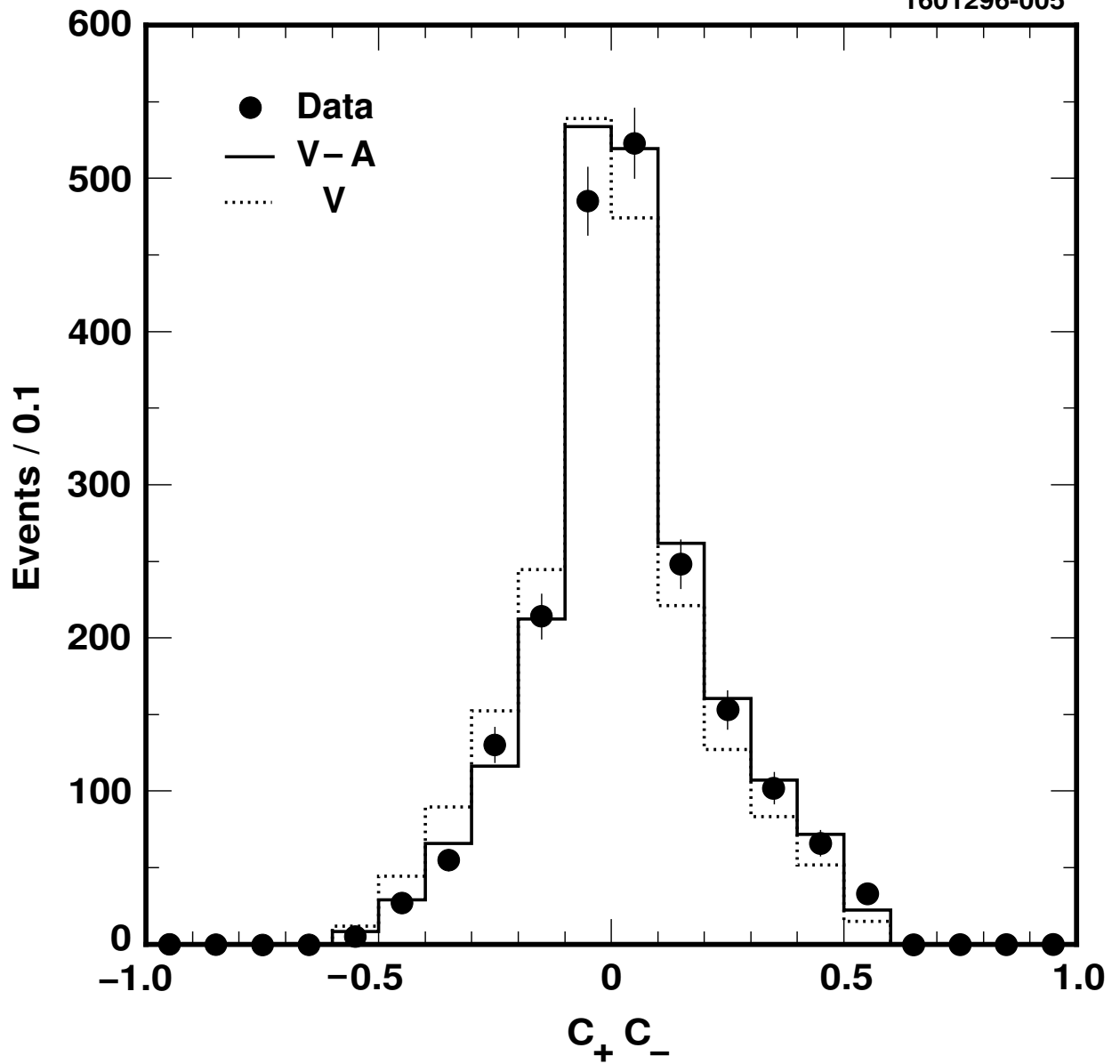


FIG. 2. The distributions of  $c_+ c_-$  for data and for  $V-A$  and  $V$  simulations.

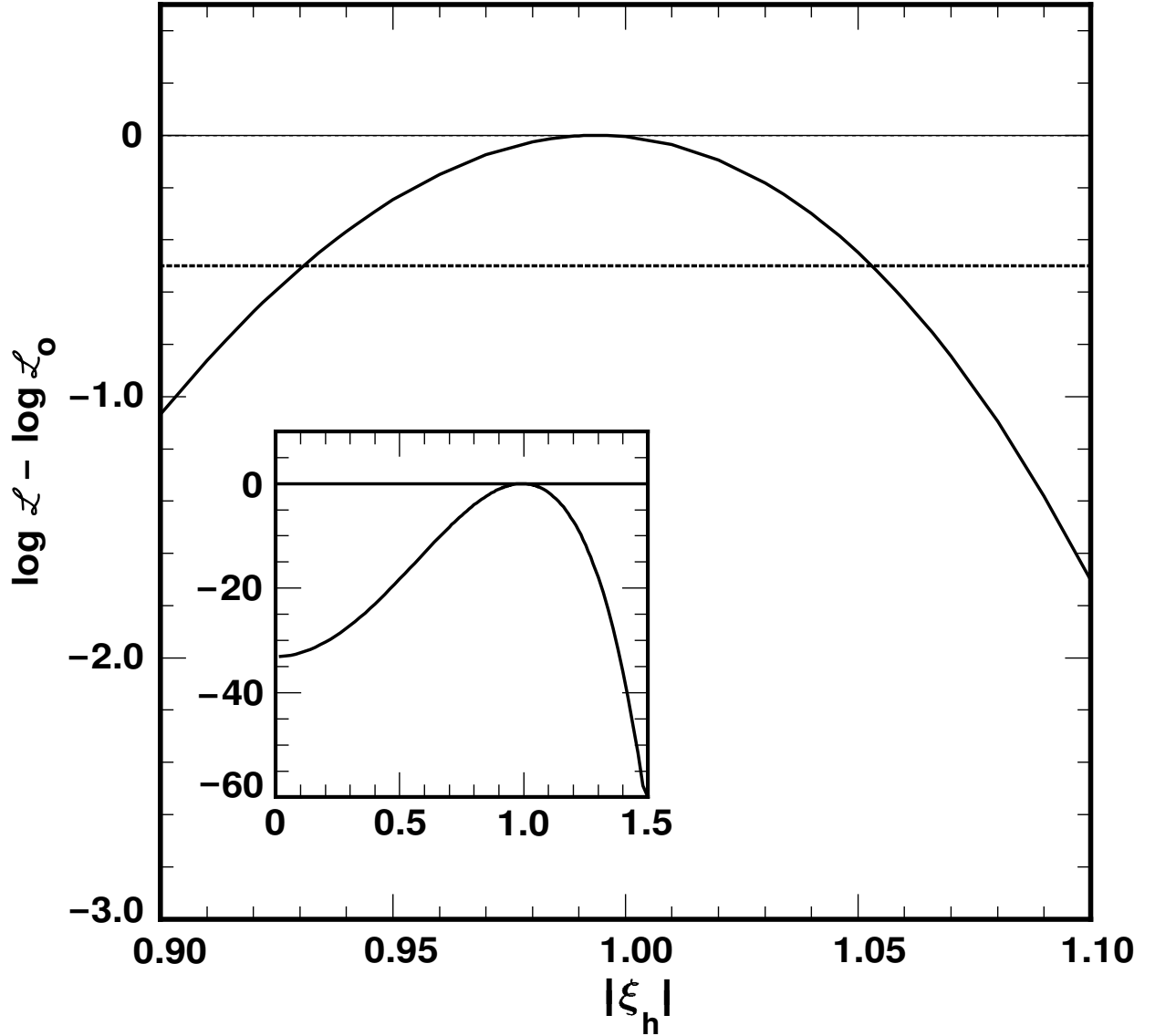


FIG. 3. Log likelihood *vs.*  $|\xi_h|$  for the  $(x_+, x_-)$  analysis. The maximum log likelihood value has been subtracted. The insert shows the full range explored.